

Effects of Machining Parameters on Cutting Force of Endmilling of Inconel 718 Using Wavy-Edge Bull-Nose Helical End-Mill under Minimum Quantity Lubrication

Doi: [10.62341/istj/12453713](https://doi.org/10.62341/istj/12453713)

Abdulahakim Ali Sultan

Administration of scientific research, The Higher Technical Center for Training and
Production- Tripoli, Libya
A.sultan@tpc.ly

1. Abstract.

This paper investigates effects of machining parameters: cutting speed (CS), feedrate (FR), and axial depth of cut (DC), on cutting force of endmilling of Inconel 718. A Wavy-edge bull-nose helical endmill (WEBNHE) was simulated cutting this material, at different levels of these parameters, then the maximum values of cutting force components (F_{xMax} , F_{yMax} , F_{zMax}), as well as the resultant (F_{Max}) were predicted using a mechanistic cutting force prediction model developed and cited from references [1-3]. The mechanistic model predicts the cutting force based on instantaneous cross-sectional area of the chip, and the local differential cutting-edge length, whereas minimum quantity lubrication (MQL) cooling strategy was incorporated into the mechanistic model via experimentally-identified cutting force and edge force coefficients which were identified and cited from the reference [4]. The simulated experimental runs in this research were designed based on Full-factorial principle, whereas MATLAB was used to simulate the mechanistic model and predict the cutting forces. The results showed that depth of cut contributed the most (by 78.94%) on the predicted resultant force (F_{Max}), Followed by Feedrate, which contributed by 20.56%, and last was the cutting speed which contributed only by 7.13%. Results also showed that, increasing feedrate and depth of cut resulted in increasing the three cutting force components and the resultant, Whereas increasing the cutting speed resulted in decreasing the F_{xMax} and F_{yMax} , but increasing the F_{zMax} . Furthermore, by focusing on the axial force component (F_{zMax}), it was observed that the effect of cutting speed was completely reversed when the feedrate reached 41 mm/min and depth of cut reached 25 mm. At these conditions, cutting speed 93 produced more F_{zMax} than 62. This can be justified by the wavy-cutting edge affecting cutting force direction.

Keywords: Wavy-edge bull-nose helical endmill; Mechanistic cutting force prediction model; Minimum Quantity Lubrication; Inconel 718; Machining parameters.

الملخص

هذه الورقة تحقق في تأثير متغيرات القطع: سرعة القطع ومعدل التغذية وعمق القطع، في قوة القطع الناتجة من عمليات التفرز لسبيكة الانكونيل 718. تمت عملية محاكاة أداة تفرز جانبي ذات حدود قطع حلزونية متموجة، ومستديرة حافة

وجهها وهي تقوم بتفريز هذه السبيكة عند مستويات مختلفة لمتغيرات القطع، ثم التنبؤ بالمركبات السينية والصادية والعينية (F_{xMax} , F_{yMax} , F_{zMax}) وكذلك المحصلة (F_{Max}) (المتغير التابع) لقوة القطع الناتجة من هذه العملية باستخدام النموذج الميكانيكي للتنبؤ بقوة القطع، والذي تم تطويره واقتباسه من بحوث سابقة [3-1]. يقوم النموذج الميكانيكي بالتنبؤ بقوة القطع على أساس مساحة المقطع اللحظية للرائش المقطوع، والطول الفرقي للحد القاطع، كذلك يأخذ النموذج في الاعتبار تأثير استراتيجية التبريد بالسوائل القليلة (MQL) في عملية التفريز من خلال ادخال معاملات القطع، ومعاملات الحد قاطع التي تم الحصول عليها تجريبيا واقتباسها من بحث سابق [4]. لقد تم تصميم التجارب في هذا البحث على أساس "العدد الكلي للتجارب"، كما تم محاكاة النموذج الميكانيكي والتنبؤ بقوة القطع باستخدام برنامج الماتلاب. لقد أظهرت النتائج ان عمق القطع أسهم بالنسبة الأعلى (78.94%) في قوة القطع المحصلة، يليه مقدار التغذية والذي أسهم بنسبة 20.56%، ثم أخيرا سرعة القطع والتي أسهمت فقط (7.13%). كما أظهرت النتائج أيضا أن زيادة كلا من مقدار التغذية وعمق القطع ادي الي ارتفاع مركبات القوة الثلاثة (F_{xMax} و F_{yMax} و F_{zMax}) والمحصلة، بينما ادي زيادة سرعة القطع الي انخفاض القوة بالمركبين F_{xMax} و F_{yMax} والمحصلة F_{Max} وارتفاعها بمركب F_{zMax} . لوحظ أيضا أن تأثير سرعة القطع قد انعكس تماما عندما ارتفع معدل التغذية الي 41 مم / دقيقة وارتفاع عمق القطع الي 25 مم، حيث انتجت سرعة القطع 93 قوة اعلي للمركب F_{zMax} من تلك التي انتجتها 62. ان هذا يمكن تبريره بإعادة توزيع القوة على المركبات الأخرى والذي سببه التموج الحاصل في حدود قطع الأداة.

الكلمات الدالة: أداة التفريز الجانبية الحزونية والتموجة حواف حدود قطعها، النموذج الميكانيكية للتنبؤ بقوة القطع، استراتيجية التبريد قليلة السوائل، سبيكة الانكونيل 718، متغيرات القطع

2. Introduction

Machining of hard-to-cut alloys such as Inconel 718 still experiences difficulties due to their exceptional properties like high shear strength, extraordinary wear resistance, work-hardening capability, low thermal conductivity, and high capability to adhere on cutting edges[3]. When machining these alloys, machining parameters such as cutting speed, depth of cut, and feedrate, have to be accurately selected and applied, whereas factors (effects) like tool design (tool geometric parameters) as well as the cooling medium and approach (cooling strategy) have to be considered as well. Otherwise, a premature failure of the cutting tool or low rate of metal removal (lower productivity) is certainly expected. Compromising between machining parameters, tool geometry and cooling strategy to optimize machining efficiency of these alloys are not always easily reachable. The optimum efficiency takes countless number of experiments and efforts to be figure out and reached. Therefore, researchers have been searching for less-cost and less-effort approaches to achieve maximizing metal removal rates and improve qualities. Group of researchers developed some mathematical modeling to modulate the machining processes and predict results, where others used computer simulation programs to simulate the processes (effortlessly) and give results.

Cutting force is a clear indication that may reflect the optimum compromising between the machining parameters, tool design, and cooling medium. The resulted cutting force of any machining operation, used specific tool, under a certain cooling strategy, indicates how far from the optimum conditions the machining parameters were selected. Cutting force can be measured directly during the machining operation, or it may be predicted using some mathematical, and math-empirical tools. In literature, there are many research studies worked on cutting force prediction, and good results were concluded and published[1-10]. One of them is a research study conducted by Kuo et al[7] in which they developed a mechanistic model to predict three responses: cutting force, surface finish, and temperature, of endmilling of Inconel 718 using ball helical endmill under dry and wet cutting conditions. Their mathematical model incorporated the effects of machining parameters on the three responses.

Using a geometric-complicated cutting tool like wavy-edge bull-nose helical endmill (WEBNHE) has become very common recently. This type of endmills was produced primarily to improve machining dynamics. It was designed to suppress (or minimize) self-excited vibrations in rough and finishing endmilling operations[1-10]. This type of tools has not gotten enough research attention in literature. Yet, few research investigated the performance of WEBNHE. Zheng et al[10] published a study in which they developed a model to predict cutting force of waved-edge end milling tool based on the relationship between the local chip thickness and the cutting-edge width. The researchers considered only the effect of shearing mechanism of cutting edges in cutting force calculation. They verified their model by endmilling of Aluminum 7075-T6 using two waved-edge cutters with different configuration. All machining parameters, material properties, and endmill/work geometry were considered in their model. Altintas et al [6] developed a discrete-time model of dynamic milling systems to predict chatter stability and cutting forces of wavy-cutting edge endmill (they called it “variable pitch and helix angle tool”). Their model was is experimentally validated in down milling of Aluminum 7050, and the tool was engaged by 5% radial immersion, and 30mm axial depth of cut, with a four-flute helical endmill. Okafor and Sultan published a study [1] in which a mechanistic model was developed to predict cutting force of endmilling of Inconel 718 using WEBNHE under emulsion (EM) cooling strategy. The study considered the shearing and ploughing mechanisms in cutting force prediction, whereas the effect of EM cooling strategy was incorporated via cutting force and edge force coefficients. Their mechanistic model was validated by several endmilling experiments on Inconel 718.

Minimum Quantity Lubrication (MQL) is a cooling and lubrication strategy in which a very small amount of biodegradable vegetable oil (lubricant) is sprayed out in forms of aerosol, using pressurized gas, toward cutting zones. Special-designed nozzles were used for this cooling strategy[3, 9]. The sprayed aerosol is a mixture of gas and oil, whereas the gas is functioning as a coolant and chip removal, however, the oil, provides lubrication and cooling effect by droplets evaporation[3]. The applied air pressure in this strategy varies from 4 to 6.5 Kg/cm², and the lubricant flow ranges from 6 to 100 ml/h[3, 9]. The air is sometimes replaced by a cooled carbon dioxide or liquid Nitrogen to improve the efficiency[4, 8]. This cooling strategy has become very popular, and it was applied by many manufacturing companies due its high efficiency, harmless to environment, beside some other advantages. However, MQL

still experience difficulties with some machining operations especially those deals with difficult-to-cut materials such as Inconel and Titanium. In fact, the strategy failed sometimes to dissipate most of the heat generated during these operations, which led to premature failures of the cutting tools, and deteriorate the surface of the workpieces[9]. Reviewing the literature has come up with few researches interested in utilizing WEBNHE, under MQL cooling strategy. Sultan and Okafor[2] investigated the effects of WEBNHE geometric parameters on predicted cutting force. They used their previously-published mechanistic model[1] to investigate effects of geometric parameters of wavy cutting edges such as wave length, wave magnitude, axial shift, and helix angle, on cutting force magnitude and direction. The study incorporated effects of MQL cooling strategy as well. Sultan and Okafor [3] also compared efficiencies of two cooling strategies: Emulsion (EM) and MQL in end-milling of Inconel 718 using a WEBNHE. Despite all previously-mentions research studies, WEBNHE still need more investigation and research.

This research work was dedicated to investigate the effects of cutting speed, axial depth of cut, and feed rates, machining parameters on cutting forces of endmilling of Inconel 718 using WEBNHE under MQL cooling strategy. The forces were predicted using a mechanistic cutting force prediction model developed by Sultan and Okafor[1-3]. A MATLAB code was used to simulate the mechanistic model under different levels of machining parameters. Three components of cutting forces were analyzed, correlations were derived, and interpretations were concluded.

3. Mechanistic Cutting Force Prediction Model of WEBNHE

WEBNHE was designed to reduce self-excited vibration (chattering) that arises with most high-speed endmilling operations. It is a special-designed wavy-helical endmill whose cutting edges are shaped in forms of 3D piecewise functions of two parts: helical and sinusoidal or wavy-helical. Fig1. depicts WEBNHE engaged in endmilling of Inconel 718, at axial immersion (depth of cut) of (a_a) and radial immersion of (a_r)[1].

To predict cutting force of this endmilling operation and cutting tool, an accurate geometric representation of the endmill, as well as a precise evaluation of cutting force and edge force coefficients are needed. The geometry is represented mathematically, whereas the coefficients are evaluated experimentally taking into account MQL cooling strategy. Okafor and Sultan [1] developed a mechanistic cutting force prediction model for WEBNHE in which they axially dissected the endmill into infinitesimal differential segments to define endmill's geometry as shown in Fig2. Then, they defined the geometry by an arbitrary point (P_{ij}), which represented the instantaneous location of every segment based on its axial location (i) and radial location (j). By defining the instantaneous location, they could calculate instantaneous chip thickness ($h_{c_{ij}}$).

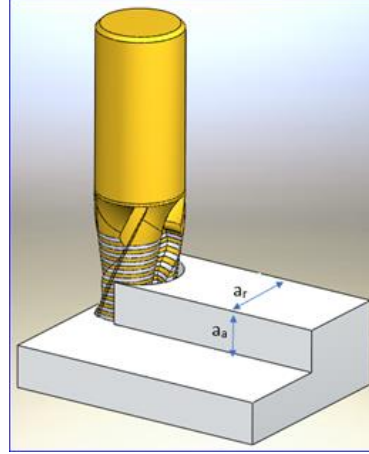


Fig1. WEBNHE engaged in endmilling of Inconel 718

By calculating the instantaneous chip thickness, they were able to calculate the instantaneous chip cross-sectional area, which was calculated by multiplying instantaneous chip thickness (h_{cij}) by chip width (db) as showing in Fig2. Finally, the chip cross-sectional area was multiplied by the identical cutting force coefficient (see Eq 1 in Fig. 2) to produce the first part of the cutting force prediction equation. This part is called “a shearing mechanism” (or shearing effect). The second part is called a “Ploughing mechanism” (or ploughing effect), and it was calculated by multiplying the differential cutting edge length (dS) by the identical edge-force coefficient. The three differential cutting force components in tangential, radial and axial directions (dF_t , dF_r and dF_a) resulted from Eq1. were projected onto the three axes (x, y, and z) using Eq.2 to get the three differential force components (dF_x , dF_y , and dF_z).

	Ploughing Mechanism	Shearing Mechanism
$dF_t(\phi_j, z_t) =$	$k_{te} dS$	$+ k_{tc} h_{cij} . db$
$dF_r(\phi_j, z_t) =$	$k_{re} dS$	$+ k_{rc} h_{cij} . db$
$dF_a(\phi_j, z_t) =$	$k_{ae} dS$	$+ k_{ac} h_{cij} . db$

(1)

Fig2. axial dissection of WEBNHE and differential force components exposed on each segment[1]

$$\begin{bmatrix} dF_x \\ dF_y \\ dF_z \end{bmatrix} = \begin{bmatrix} -\cos(\phi_{ij}) & -\sin(\phi_{ij}) \sin(k_{ij}) & -\sin(\phi_{ij}) \cos(k_{ij}) \\ \sin(\phi_{ij}) & -\cos(\phi_{ij}) \sin(k_{ij}) & -\cos(\phi_{ij}) \cos(k_{ij}) \\ 0 & -\cos(k_{ij}) & -\sin(k_{ij}) \end{bmatrix} \begin{bmatrix} dF_t \\ dF_r \\ dF_a \end{bmatrix} \quad (2)$$

The total cutting force for each cutting edge can be calculated by integrating the differential cutting force components (df_x , df_y , and df_z) along the cutting edges using Eq. 3

$$\begin{aligned} F_x(\phi_{ij}) &= \sum_{i=1}^{N_t} \int_0^{a_a} dF_x \{ \phi_{ij}(z_t, k_{ij}) \} \cdot dz \\ F_y(\phi_{ij}) &= \sum_{i=1}^{N_t} \int_0^{a_a} dF_y \{ \phi_{ij}(z_t, k_{ij}) \} \cdot dz \\ F_z(\phi_{ij}) &= \sum_{i=1}^{N_t} \int_0^{a_a} dF_z \{ \phi_{ij}(z_t, k_{ij}) \} \cdot dz \end{aligned} \quad (3)$$

Substituting Eq.2 into Eq.3 yields Eq.4 as following:

$$\begin{aligned} F_x(\phi_{ij}) &\left\{ \sum_{j=1}^{N_t} \int_0^{a_a} [-dF_t \cos(\phi_{ij}) \quad -dF_r \sin(\phi_{ij}) \sin(k) \quad -dF_a \sin(\phi_{ij})] dz \right\} \\ F_y(\phi_{ij}) &\left\{ \sum_{j=1}^{N_t} \int_0^{a_a} [-dF_t \sin(\phi_{ij}) \quad -dF_r \cos(\phi_{ij}) \sin(k) \quad -dF_a \cos(\phi_{ij})] dz \right\} \\ F_z(\phi_{ij}) &\left\{ \sum_{j=1}^{N_t} \int_0^{a_a} [0 \quad -dF_r \cos(k_{ij}) \quad -dF_a \sin(k)] dz \right\} \end{aligned} \quad (4)$$

Ameen[4] conducted experimental work to evaluate the cutting force coefficients and edge force coefficients, and to validate the mechanistic model for Okafor and Sultan[1]. Fig3. illustrates the flow chart of cutting force prediction using Okafor and Sultan's mechanistic model (the green path), and also illustrates Ameen's experimental validation work (brown path) used to validate the mechanistic model of Okafor and Sultan and to predict the forces.

Both the mechanistic cutting force prediction model of Okafor and Sultan as well as Ameen's experimental validation work were used in this study to investigate effects of machining parameters on cutting force prediction of endmilling on Inconel 718 using WEBNHE.

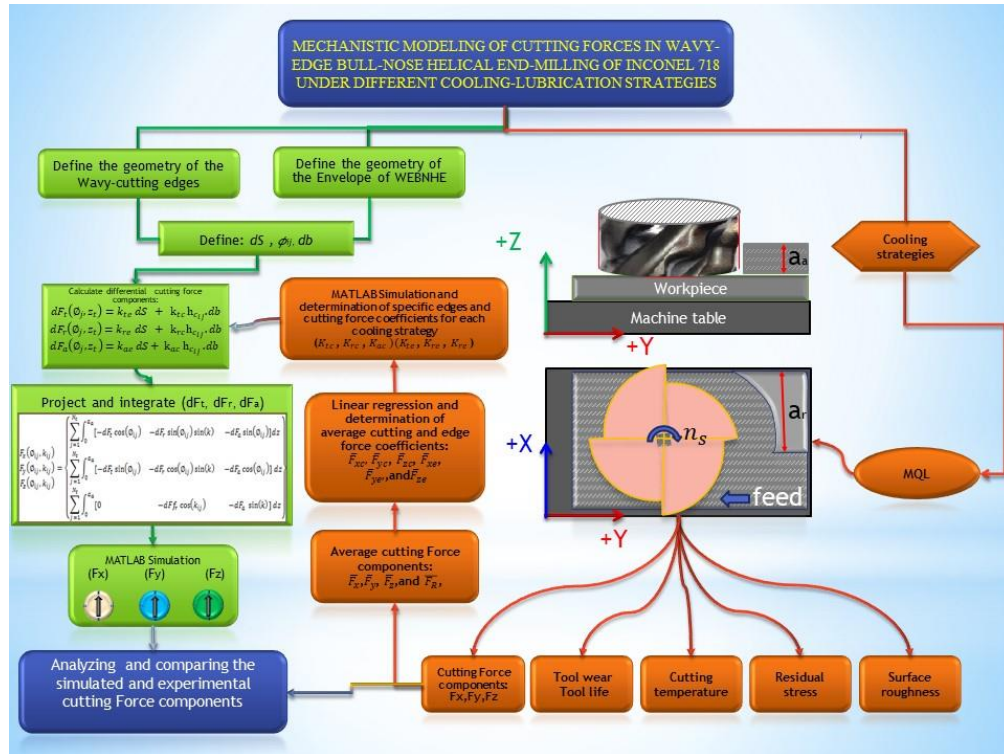


Fig3. Flow chart of the mechanistic cutting force prediction model and flow of experimental work to calculate cutting force and edge force coefficients

4. Experimental Setup

Six- flutes WEBNHE of 1.25" (31.75mm) diameter was selected to simulate the endmilling of Inconel 718 under MQL cooling strategy. The endmill was in full radial immersion which means the whole diameter was engaged in the cutting. The investigated machining parameters were selected as two Cutting speeds (CS) of 62 and 93 rpm, three feedrate (FR) of 27, 41, and 56 mm/min, and five of depth of cut (DC) of 5, 15, 25, 35 and 45 mm. All the levels were selected based on the manufacturer's recommendations. Cutting force coefficients and edge force coefficients (See Tab1) applied in this simulation are quoted from the study of Ameen[4].

Table1. Cutting force coefficients and edge force coefficients used in this study[1]

CS (rpm)	k_{te} N/mm ²	k_{re} N/mm ²	k_{ae} N/mm ²	k_{te} N/mm	k_{re} N/mm	k_{ae} N/mm
62	2604	-4948	-76.26	31.42	-35.2	-6.92
93	3328.6	-5348	-515.87	12.79	-25.8	0.036

The experimental work setup, predicted maximum cutting force components, as well as the maximum resultant cutting force are illustrated in Tap2 which shows 30 experimental runs applying all the machining parameters. A mathematical algorithm developed by Sultan and Okafor [1-3] was used to simulate the 30 runs. A MATLAB software Ver. 2016 was used to execute the Algorithm and predict the cutting force components and the resultant cutting force of each run. The simulation process was executed for one-revolution endmilling (2π or 360°). The one-revolution was divided into steps, at every step the Algorithm stops and calculate the force components and the resultant along the whole axial immersions of parts of cutting edges engaged in the cutting, then plot them onto graphs.

5. Results and Discussion

One-revolution (2π or 380°) of the WEBNHE endmilling of Inconel 718 under MQL was simulated, and cutting force components (F_x , F_y , F_z), as well as the resultant cutting force (F) were predicted. Fig4. illustrates (F_x , F_y , F_z , and F) predicted at 93 rpm, 27mm/min, and 5mm).

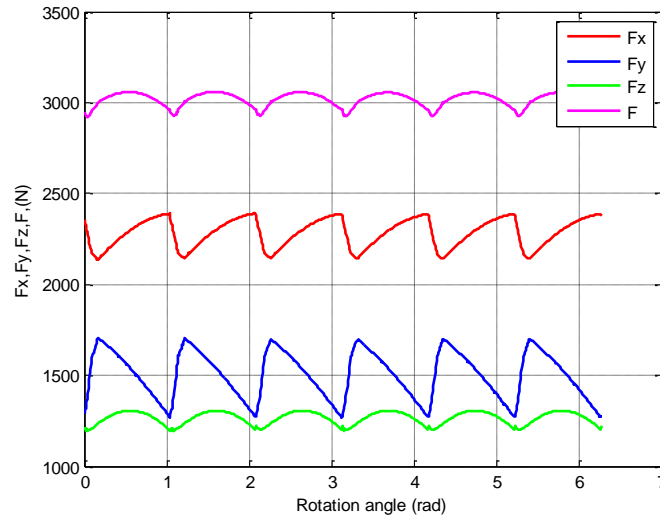


Fig4. F_x , F_y , F_z , and F predicted from one- Revolution simulation of WEBNHE endmilling at 93 rpm, 27mm/min, and 5 mm).

Fig4, clearly, shows six peaks of the cutting force, which represent the six cutting edges of the WEBNHE. In terms of magnitude, F_x (the force component normal to the feed direction) was the highest, followed by F_y (the force component directed in the feed direction), later was F_z . This result agreed with what was published in [1-3].

Tab3. shows the maximum values of cutting force components and the maximum resultant cutting force (F_{xMax} , F_{yMax} , F_{zMax} and F_{Max}) of all the simulated runs. To study the effect of the machining parameters on the predicted cutting force components, a multiple regression analysis was conducted, and a regression model was developed. The analysis exhibited the relationship between F_{max} (response) and the machining parameters (predictors): Cutting speed (CS), Feedrate (FR), depth of cut (DC), and their interactions: CS/FR, CS/DC, and FR/DC. The developed model shown “P” value less than 0.001 which denote that the factors were statistically significant, and R-sq of 99.90% which means that 99.90% of the variation in F_{Max} can be explained by this regression model. Eq.5 is the the regression equation developed by the analysis.

$$F_{Max} = -12871 + 173.1 (CS) + 339.8 (FR) + 760.5 (DC) - 4.339 (CS)(FR) - 8.690 (CS)(DC) + 19.887 (FR)(DC) \quad (5)$$

Despite of the two data points that have large residuals, and the small sample number of runs ($n=30$), some machine parameters have added values to the equation: DC alone added the most-71.5%, whereas adding FR and CS improved the equation to 87 % and 92.37% respectively. The interaction effects of the three parameters have additionally improved the equation up to 99.87%.

5.1 Effects of Machining parameters on F_{Max}

Fig5 and Fig 6 demonstrate how machining parameters affected the F_{Max} , and interacted with each other during the experimental runs. Results of the regression model showed that DC contributed (the most) by 78.94% in F_{Max} , Followed by FR, which contributed by 20.56%, Whereas CS contributed only by 7.13%. Figs 5&6 showed that increasing in CS from 62 to 93rpm has decreased the F_{Max} from 26878 to 19951N, whereas increasing FR from 27 to 56mm/min has increased the F_{Max} from 16239 to 30758N. Additionally, increasing DC from 5mm to 45mm has also increased the F_{Max} from 5080 to 41579N.

In terms of interacting the machining parameters with each other, and the cutting force, Fig5 demonstrates that very likely interactions were occurred especially in cases of DC /CS, and DC/FR. For instance, rising the DC, from 25 up to 35 then to 45 mm under 93rpm resulted less rising proportion in cutting force than rising the same parameter under 62rpm. The process can be optimised in this point and get advantage of it. The case FR/CS is less likely to have interaction meaning that changing CS with FR have same effect in two CS leves. Tab2. Show five recommended endmilling runs proposed by the regression model because its was determined to the model that the objective was to minimize the F_{Max} . However, maximizing the marching parameters is another goal of machinists, However, they have to compromise between minimizing the cutting force and maximizing machining parameters, which depends on other factors like rigidity of the machine and the properties of cutting tool material.

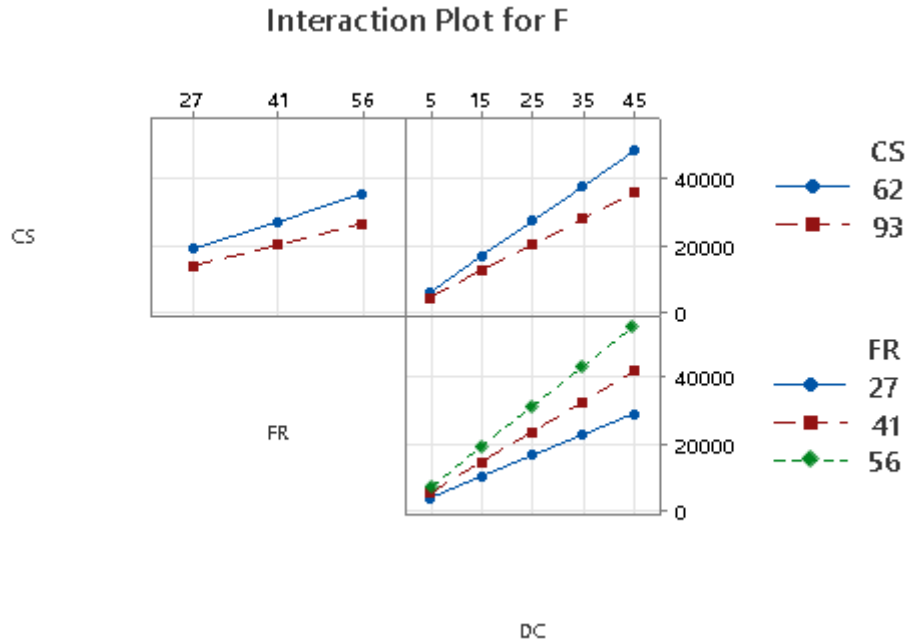


Fig5. Effects of interaction of CS, FR, and DC on F

Tab2. Five recommended runs proposed by the regression model

CS	FR	DC	Predicted Fmax
93	27	5	3953.69
93	41	5	4453.17
93	56	5	4988.33
62	41	5	5948.05
62	56	5	8500.75

Tab3. F_{xMax} , F_{yMax} , F_{zMax} and F_{RMax} (response) predicted at two levels of CS (62 and 93rpm), three levels of FR (27, 41, and 56mm/min), and five levels of DC (5,15,25,35, and 45mm)

Run Order	Cutting speed (RPM)	Feedrate (mm/Min)	Depth of Cut (mm)	F_{xMax} (N)	F_{yMax} (N)	F_{zMax} (N)	F_{Max} (response) (N)
1	62	27	5	3441.55	2418.04	1751.41	4253.08
2	62	27	15	10134.99	6376.62	2160.43	11664.79
3	62	27	25	16262.52	9923.10	2512.35	18790.15
4	62	27	35	22514.08	13557.11	2874.98	25904.99
5	62	27	45	28745.96	17163.82	3263.83	33087.41
6	62	41	5	4700.02	3159.16	2300.54	5807.80
7	62	41	15	14360.77	8784.76	2763.82	16517.32
8	62	41	25	23329.91	13794.99	3168.39	26751.99
9	62	41	35	32327.52	18826.23	3587.87	36969.41
10	62	41	45	41295.51	24022.65	4032.09	47386.21
11	62	56	5	6048.71	3953.21	2888.90	7475.35
12	62	56	15	18888.38	11367.19	3410.32	21728.43
13	62	56	25	30902.12	17943.44	3871.60	35290.12
14	62	56	35	42841.91	24487.30	4354.08	48838.03
15	62	56	45	54884.29	31371.40	4855.22	62716.83
16	93	27	5	2390.26	1704.58	1305.44	3059.30
17	93	27	15	7232.38	4713.97	1800.46	8582.43
18	93	27	25	11737.22	7379.71	2262.23	13768.01
19	93	27	35	16203.85	10121.99	2752.44	18982.10
20	93	27	45	20694.20	12908.01	3215.50	24301.63
21	93	41	5	3320.00	2336.09	1798.42	4286.10
22	93	41	15	10315.91	6752.45	2550.84	12318.79
23	93	41	25	16869.77	10659.83	3252.71	19846.56
24	93	41	35	23310.53	14611.64	3997.76	27411.28
25	93	41	45	29874.09	18733.66	4701.64	35169.20
26	93	56	5	4316.15	3012.71	2326.61	5600.69
27	93	56	15	13632.12	8937.33	3354.81	16322.86
28	93	56	25	22368.94	14174.25	4313.95	26359.45
29	93	56	35	30924.83	19434.33	5332.05	36442.68
30	93	56	45	39709.67	24975.42	6293.94	46813.71

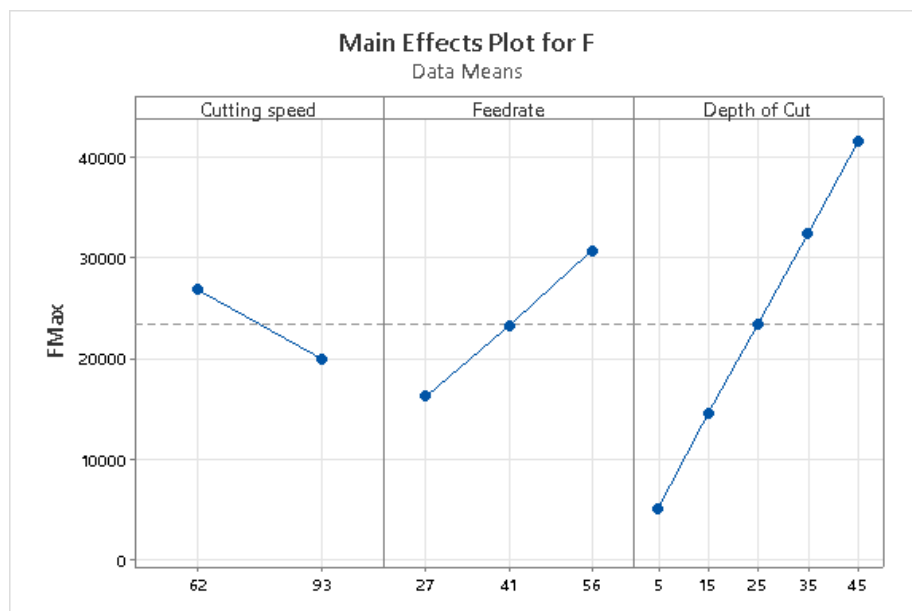
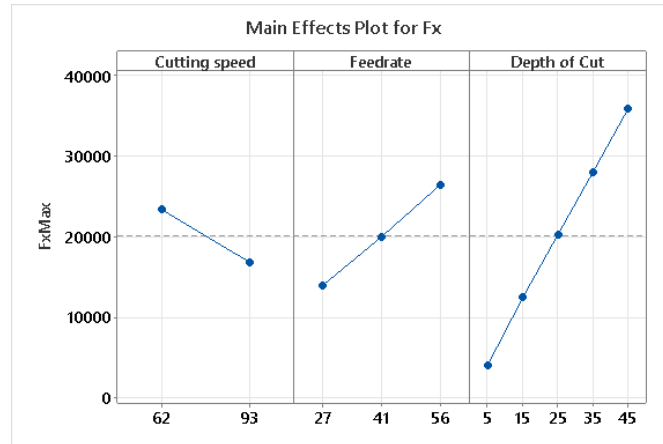


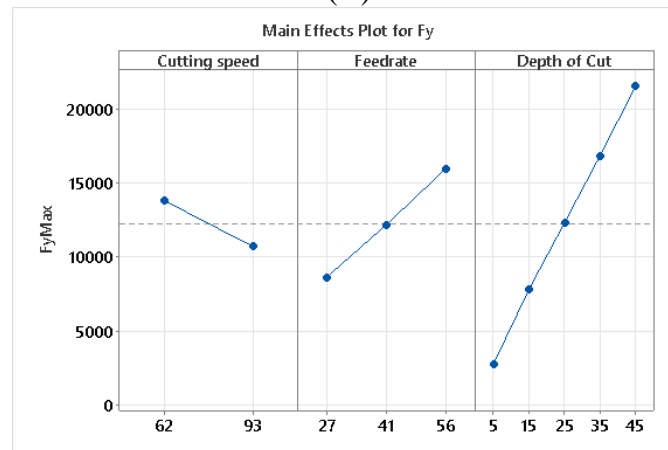
Fig6. Effect of CS, FR, and DC on F_{max}

5.2 Effects of CS, FR, DC, CS/FR, CS/DC on F_{xmax}, F_{yMax}, and F_{zMax}

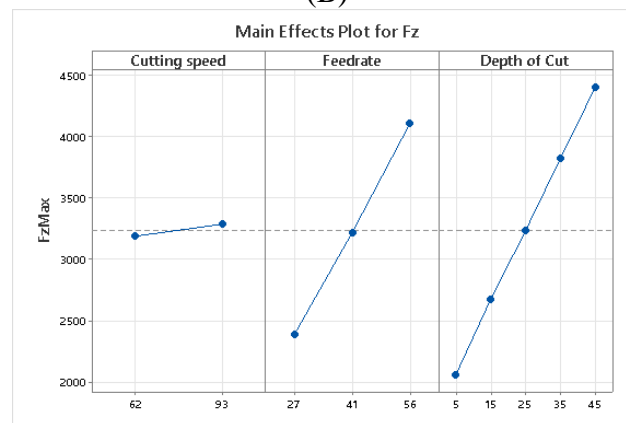
Studying the effects of cutting parameters on cutting force components show what component was affected the most (or the least) by which parameter. Fig 7(A, B, and C) shows effects of CS, FR, DC on F_{xMax}, F_{yMax}, and F_{zMax}. It is obvious that FR and DC affected the three force components in a very similar way, that is when FR and DC increased, F_{xMax}, F_{yMax}, and F_{zMax} were all increased although the increasing rates of the three components were not equal (see Fig7). A drastic increase in F_{xMax} and F_{yMax} (13093N, 7339 respectively) were caused by FR increase from 27 to 56mm/min. Whereas, a drastic increase in F_{xMax} and F_{yMax} (31831N, 18766 respectively) were caused by DC increase from 5 to 45mm. it is worthy to point out that those two force components (F_{xMax} and F_{yMax}) are oriented into feed direction, and normal-to-feed directions (respectively) of the tool (WEBNHE), which means this drastic increase would tend to deflect the tool radially and may vibrate it as well during the machining. Therefore, the operator has to consider this in workpiece setup as well as the type of machine to be used. CS, however, was dissimilar to FR and DC. when CS increased from 62 to 93rpm, F_{xMax} decreased from 23378N to 16860N and F_{yMax} decreased from 13809N to 10697N, F_{zMax} increased from 3186N to 3283N. What interesting is that at FR>41mm/min, and DC>25mm, the 62rpm produced less F_{zMax} than 93rpm, as illustrated in Fig8 which shows interaction effects of cutting parameters on cutting force components. This could be justified by the effect of the wavy-profile of cutting edges whereas some portion of cutting forces were subtracted from F_{xMax}, F_{yMax} and undertaken by F_{zMax}, which is not a problem as this component is directed in axial orientation of the tool.



(A)



(B)



(C)

Fig7. Effect of CS, FR, and DC on F_{xMax} , F_{yMax} , and F_{zMax}

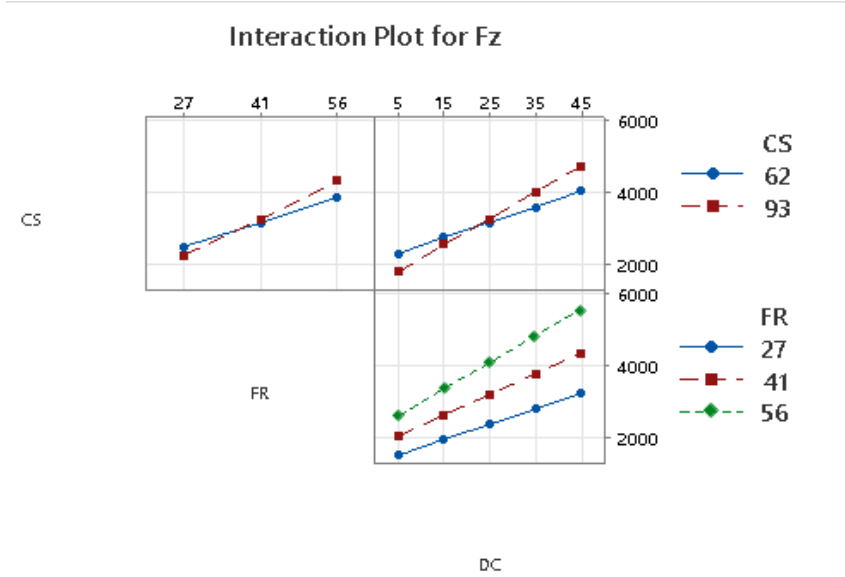


Fig8. Effects of interaction of CS, FR, and DC on $F_{z_{max}}$

6. Conclusion

Effects of cutting parameters cutting speed, feedrate, and depth of cut on predicted cutting force components were investigated, and concluding observations and remarks were extracted as following:

- 1) A study to investigate the effect of cutting speed, feedrate, and axial depth of cut on predicted cutting force of end-milling of Inconel 718 using Wavy-edge bull-nose helical endmill (WEBNHE), under a Minimum Quantity Lubrication (MQL) has been conducted.
- 2) A regression model has been developed to study the effect of the machining parameters on the cutting forces of the endmilling processes.
- 3) It was observed that that depth of cut contributed by 78.94% in F_{max} , Followed by feedrate, which contributed by 20.56%, whereas cutting speed contributed only by 7.13%.
- 4) Results have also shown that increasing in cutting speed from 62 to 93rpm has decreased the F_{max} from 26878N to 19951N, whereas increasing feedrate from 27mm to 56mm/min has increased the F_{max} from 16239N to 30758N. Additionally, increasing depth of cut from 5mm to 45mm has also increased the F_{max} from 5080N to 41579N.
- 5) A drastic increase in $F_{x_{max}}$ and $F_{y_{max}}$ (31831N, 18766 respectively) were caused by DC increase from 5 to 45mm, and a drastic increase in $F_{x_{max}}$ and $F_{y_{max}}$ (31831N, 18766 respectively) were caused by DC increase from 5 to 45mm. These two components are radially-oriented cutting force components.
- 6) Results also demonstrated that at $FR > 41$ mm/min, and $DC > 25$ mm, the 62rpm produced less $F_{z_{max}}$ than 93rpm.

7. Acknowledgment

The author would like to express special and sincere gratitude and thankfulness to Dr. Ahmed Eshibli, and Mr. Adel Elshreef for their collaboration and help with the statistics and regression model.

8. References

- [1] A. C. Okafor and A. A. Sultan, "Development of a mechanistic cutting force model for wavy-edge bull-nose helical end-milling of inconel 718 under emulsion cooling strategy," *Applied Mathematical Modelling*, vol. 40, no. 4, pp. 2637-2660, 2016.
- [2] A. A. Sultan and A. C. Okafor, "Effects of geometric parameters of wavy-edge bull-nose helical end-mill on cutting force prediction in end-milling of Inconel 718 under MQL cooling strategy," *Journal of Manufacturing Processes*, vol. 23, pp. 102-114, 2016.
- [3] A. A. Sultan and A. C. Okafor, "Investigating the efficiency of minimum quantity lubrication and emulsion cooling strategies in endmilling of Inconel 718 using wavy-edge bull-nose helical endmill," *International Science and Technology Journal*, vol. 27, pp. 372-396, 2021.
- [4] M. S. Ameen, "Mechanistic identification of specific force coefficients in endmilling Inconel 718 under four cooling strategies," MECHANICAL ENG., Missouri University of Science and Technology, 2014.
- [5] C. Eksioglu, Z. Kilic, and Y. Altintas, "Discrete-time prediction of chatter stability, cutting forces, and surface location errors in flexible milling systems," *Journal of Manufacturing Science Engineering*, vol. 134, no. 6, 2012.
- [6] Y. Kaynak, "Evaluation of machining performance in cryogenic machining of Inconel 718 and comparison with dry and MQL machining," *The International Journal of Advanced Manufacturing Technology*, vol. 72, no. 5, pp. 919-933, 2014.
- [7] C.-P. Kuo, C.-C. Ling, S.-H. Chen, and C.-W. Chang, "The prediction of cutting force in milling Inconel-718," *The International Journal of Advanced Manufacturing Technology*, vol. 27, no. 7, pp. 655-660, 2006.
- [8] Y. Su *et al.*, "Refrigerated cooling air cutting of difficult-to-cut materials," *International Journal of Machine Tools*, vol. 47, no. 6, pp. 927-933, 2007.
- [9] V. Upadhyay, P. Jain, N. Mehta, and K. Branko, "Minimum quantity lubrication assisted turning—an overview," *Daaam international scientific book*, pp. 463-478, 2012.
- [10] S. Zhang, J. Li, and Y. Wang, "Tool life and cutting forces in end milling Inconel 718 under dry and minimum quantity cooling lubrication cutting conditions," *Journal of cleaner production*, vol. 32, pp. 81-87, 2012.